University of Groningen

Physics of one-dimensional hybrids based on carbon nanotubes

Gao, Jia

IMPORTANT NOTE: You are advised to consult the publisher's version (publisher's PDF) if you wish to cite from it. Please check the document version below.

Document Version
Publisher's PDF, also known as Version of record

Publication date:
2011

Link to publication in University of Groningen/UMCG research database

Citation for published version (APA):
Gao, J. (2011). *Physics of one-dimensional hybrids based on carbon nanotubes*. s.n.

Copyright
Other than for strictly personal use, it is not permitted to download or to forward/distribute the text or part of it without the consent of the author(s) and/or copyright holder(s), unless the work is under an open content license (like Creative Commons).

Take-down policy
If you believe that this document breaches copyright please contact us providing details, and we will remove access to the work immediately and investigate your claim.

Downloaded from the University of Groningen/UMCG research database (Pure): http://www.rug.nl/research/portal. For technical reasons the number of authors shown on this cover page is limited to 10 maximum.

Download date: 16-05-2021

Chapter 6

Extrinsic effects on the ambipolar electrical transport in semiconducting single-walled carbon nanotube transistors

In this chapter, we report both hole and electron transport in field-effect transistors by using high purity semiconducting single-walled carbon nanotube (SWNT) dispersion. A highly scalable method is demonstrated for the sample preparation and the resulting transistors show carrier mobility in the range of 10^{-3}*-*10^{-2} *cm*^{2}*/V s both for holes and electrons. The on/off ratio of the device (channel length 5* μ*m) is higher than* 6×10^2 *which is one of the highest reported for short channel FETs with SWNT networks. We further show the effects of air exposure on the performance of the transistors. Interestingly, the hole mobility increases with the exposure to air, while the electron mobility significantly decreases.*[*]

[*] J. Gao, I. Iezhokin, M. A. Loi, *submitted.*

6.1 Introduction

Semiconducting single-walled carbon nanotubes (SWNTs), one of the most important candidates for next generation semiconductor technology, have shown great potential as active material for field-effect transistors (FETs). [1-4] The protocols used for device fabrication can be generally described in two categories. In the first category, SWNTs are grown on a substrate by chemical vapor deposition (CVD) methods at high temperature (~900℃) and then the electrodes are patterned by electron beam lithography. The active components of the device can be either single tube or a network of them. [5-11] The resulting transistors show ambipolar behavior, which means that carbon nanotubes conduct both holes and electrons. In the second category, pristine SWNTs are dispersed in aqueous or organic solution and then deposited by solution-based methods on the substrate with pre-patterned electrodes. The second process scheme allows for large area device preparation and low temperature processing, which are certainly more suitable for further device integration. However, the electron transport in the device fabricated following this protocol, the n-type characteristic, is generally strongly suppressed or totally absent. [12-15] The origin of this electron transport deficiency is still under debate. One of the generally held views is that electron injection is obstructed due to the Schottky barriers at the metal/SWNTs interface. [16] Recently, Martel et al. demonstrated that the oxygen/water couple could electrochemically induce electrons transfer from semiconducting SWNTs to them and suppress electron conduction in SWNTs much like in organic semiconductors. [17] It is therefore desirable to explore the optimal condition for the fabrication of ambipolar FET with solution-processable SWNTs and further understand the effect on the electrical characteristics of air exposure and/or thermal annealing.

In this work, we report the preparation of ambipolar FETs with high purity semiconducting SWNT dispersion. Solution processed FETs with randomly distributed SWNT network in the channel show carrier mobility in the range of 5-8.5×10^{-3} cm^2/V s for hole transport and 2-4×10^{-3} cm^2/V s for electron transport. Moreover, the effect of the different environmental conditions on the ambipolar electrical characteristics of the FETs is reported. The hole mobility of SWNT FETs increases of 60% with exposure to air for 24 h and the threshold voltage shows a positive shift. On the contrary, the electron transport is suppressed with exposure to air and no electron transport was observed after one day in air ambience. An almost recovery of the mobility for holes was obtained by re-annealing in vacuum. While electron transport was only partially recovered, showing degraded characteristics.

Annealing in air converted ambipolar SWNT devices into unipolar ones and increased the hysteresis in transistors I-V characteristics

6.2 Results and discussion

The absorption spectra of the as-dispersed SWNTs (dash) and the one after enrichment (solid) are shown in Figure 6.1. Poly(9,9-di-n-octylfluorenyl-2,7-diyl) (PFO) solution in toluene has proven to be one of the most effective polymers for sorting semiconducting SWNTs due to the unique interaction between the polymer chains and semiconducting carbon nanotubes. [18-21]

The absorption spectrum of the as-dispersed SWNTs (dash) shows almost no background intensity, which is generally an indication of presence of bundles and of metallic tubes. The peaks at wavelength higher than 900 nm are the E_{11} transition of 4 semiconducting SWNT species corresponding to (7,5), (7,6), (8,6) and (8,7). The absorbance below 400 nm is due to the polymer chains in the solution with concentration close to that of the pristine solution (~0.3 mg/mL). The absorption spectrum of the SWNTs after enrichment (solid curve Figure 1) shows much higher absorbance intensity (O.D. ~ 0.2) than that of the as-dispersed one (O.D. ~ 0.05). By taking into account the absorption cross section $\alpha(E_{11}^{S}) \approx 1\times10^{-18}\, cm^2 / atom$ for dispersed carbon nanotubes, [22] we estimated the SWNT concentration to be about 0.4 μg/mL for the as-dispersed nanotubes and 6 μg/mL for the one after enrichment. No optical transitions from metallic species in the spectral range of 500-600 nm were observed. The reduction of absorption intensity at 380 nm is remarkable and indicates that this method is highly efficient in removing excess polymer from the dispersion.

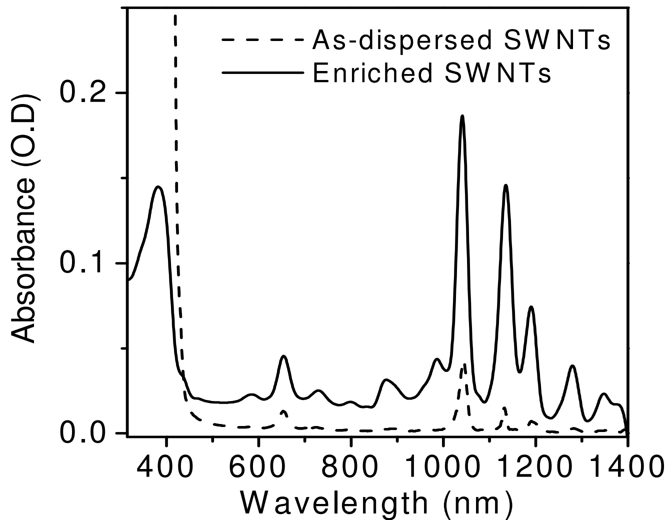

Figure 6.1 Optical absorption spectra of the as-dispersed SWNTs (dash curve) and the enriched SWNTs (solid curve) in toluene solution.

So far, there have been a couple of reports on the preparation of semiconducting SWNT dispersion by using conjugated polymers to make electronic devices. From these it appears clear that the removal of the polymer is essential to achieve good performing devices. Izard et al. reported the separation of dispersed SWNTs from the excess PFO by extensive washing. [23] However, the efficiency of the separation and the yield of the procedure for SWNT enrichment were not mentioned in details. Krupke et al. reported the realization of carbon nanotube device array by using PFO/toluene dispersed SWNTs but no efficient method for the removal of wrapped polymers was presented. [24] Recently, Chan-Park et al. demonstrated a degradable conjugated polymer for the enrichment of semiconducting SWNTs but the selectivity of the polymer is not as good as that of PFO. [25] Arnold et al. presented a method with two-step centrifugation for the preparation of semiconducting SWNTs analogues to what we used in this study. [26] However, our procedure has the advantage of being much less time-consuming than the previously reported one.

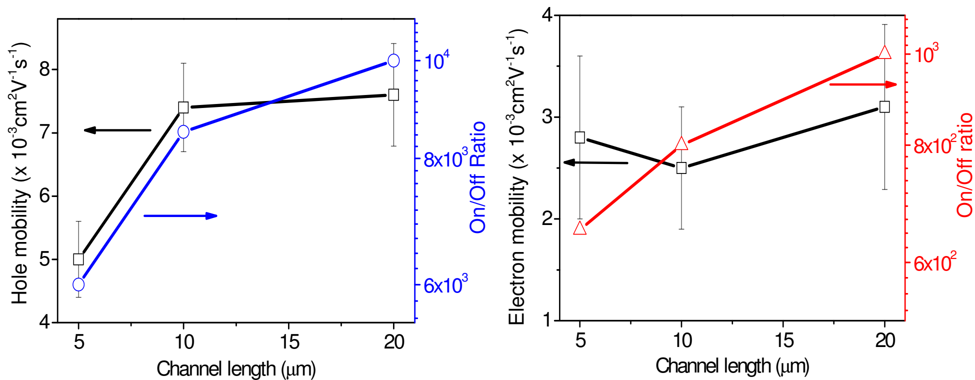

Figure 6.2 Analysis of the electrical characteristics of SWNT transistors: (a) Hole mobility and average on/off ratio versus device channel length; (b) Electron mobility and average on/off ratio versus device channel length. The error bars indicate the spread of results obtained over all the measured devices.

Figure 6.2 shows the electrical characteristics of bottom-contact FETs with randomly distributed SWNT network as channel. More than 10 devices were measured for each channel length. The carrier mobility is calculated by using the saturation regime formula for field-effect transistors as reported in the experimental section. The values for channel width (W: 1 cm) and length (L: 5, 10, 20 μm) are defined by the pattern of the electrodes. The obtained hole mobility (μ_h) is in the range of 5-8.5×10^{-3} cm^2/V s and electron mobility (μ_e) is 2-4×10^{-3} cm^2/V s. The device mobility remains almost constant with the increase of the channel length while the on/off ratio increases. The off current is in the order of 10^{-10} Ampere at source drain bias (V_d = -5 V) and on/off ratio of all the devices is in the range of 10^3-10^4 for p-channel and 6 ×10^2-10^3 for n-channel, which is comparable to that reported for a 99% semiconducting SWNT solution. [1] This data indicates the high purity of the semiconducting SWNT dispersion and is in good agreement with that estimated from optical measurements. In fact high on/off ratio with short channel length are not achievable without a metallic-tube free carbon nanotube sample.
Despite of the good on/off ratio, the overall device performance seems to be inferior to the one reported in the paper by Engel et al. [1] which reaches up to 20 cm^2/V s. However, it is important to notice that the device performance is determined by the SWNT coverage in the channel region and by the concentration of metallic tubes in the network. [27-29] For this purpose we have also calculated the effective mobility of the FETs by taking into account the nanotube coverage and not only the simple geometry of the transistor channel as for the data reported above. The details will be discussed below. However, out intention in the study is not to compete for the highest device performance but rather to understand the

characteristics of solution-processed SWNT transistor, also the influence of the environment on their transport mechanism.

One of the important characteristics of our solution-processed FETs is their ambipolar character. As we discussed above, most of solution-processed SWNT FETs so far have shown only hole conduction (unipolar) and the generally accepted views for the suppression of electron conduction include: (i) large Schottky barrier at nanotube-electrode interface impedes electron injection; (ii) the –OH groups on the surface of dielectric layer act as traps for electrons; (iii) Adsorbed H_2O and/or O_2 molecules act as redox couple and induce an electron transfer from SWNTs the molecules, leading to the suppression of the electron conduction.

The injection barrier could be ruled out as a major factor because the Schottky barrier formed at the interface between Au electrode (work function: 4.9) and carbon nanotubes with diameter around 0.9 nm (Fermi level: 4.5 eV) [30] is as high as 1 eV, and much larger than the one between Au and SWNTs with diameter larger than 1.1 nm, [31] indicating that the barrier is not the main factor for the limited electron conduction.

Conversely, it appears that the ambipolarity of SWNT transistors benefits from the surface treatment on dielectrics with 3-aminopropyltriethoxysilane (APTES) that reduced the density of –OH group, in particular when the sample preparation is done in water free environment.

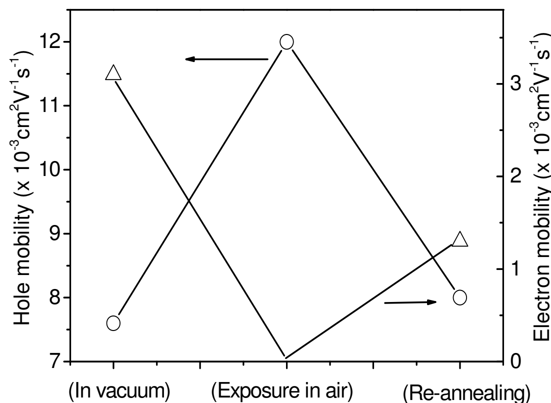

Figure 6.3 Variations of field effect mobility with exposure to ambient conditions. Solid line is drawn to guide the eyes.

In order to investigate the effects of water and oxygen on the performance of SWNT devices, we exposed the devices to ambient environment (~70% relative humidity at 20℃) for up to 24 h and performed I-V measurements under the same conditions. We observed that ambient conditions induced an increase in hole transport as well as a decrease in electron conduction of the device. Hole mobility

increased from 7.5×10^{-3} to 1.2×10^{-2} cm^2/V s after 24 h exposure and the threshold voltage (V_{th}) for the p-channel showed positive shifts (-4 V to 4 V). Simultaneously the n-channel degraded with exposure to air and no current was observed after 24 h with gate bias up to 60 V. Similar behavior have also been observed in single and double-walled carbon nanotube FETs [32, 33] and has been attributed to the effects of oxygen, such as the variation of the work function of electrode with exposure to air or the hole doping.

A mere contribution coming from change of the work function of Au electrodes is hardly enough to explain the shift of threshold voltage and the tremendous degradation of n-channel characteristics. We therefore conclude that the suppression of electron conduction in ambipolar FETs is the result of the electrochemical interaction between adsorbed molecules (water and/or oxygen) and the semiconducting SWNT, as was suggested by Martel et al. [17] The electron density in the channel decreases due to this interaction. The hole-electron recombination in semiconducting carbon nanotube thus reduced, which leads to a positive shift of the threshold voltage.

Further understanding of ambience-stability of ambipolar SWNT FETs was obtained by re-testing the exposed device in vacuum after annealing also in vacuum at 130 ℃ for 2 h. In this case we observed a general recovery of the starting performance. The hole mobility and the threshold voltage showed a similar value to the initial values (μ_h ~ 8×10^{-3} cm^2/V s and V_{th} ~ -7 V). While in the n-range the complete recovery is almost achieved with values for the electron mobility lower than the starting value (1.3×10^{-3} cm^2/V s compare to 3.1×10^{-3} cm^2/V s) and a shift of the threshold voltage towards positive direction (10 V to 30 V). Moreover, the hysteresis in I-V characteristics of the FET after re-annealing in vacuum is also larger than the starting device.

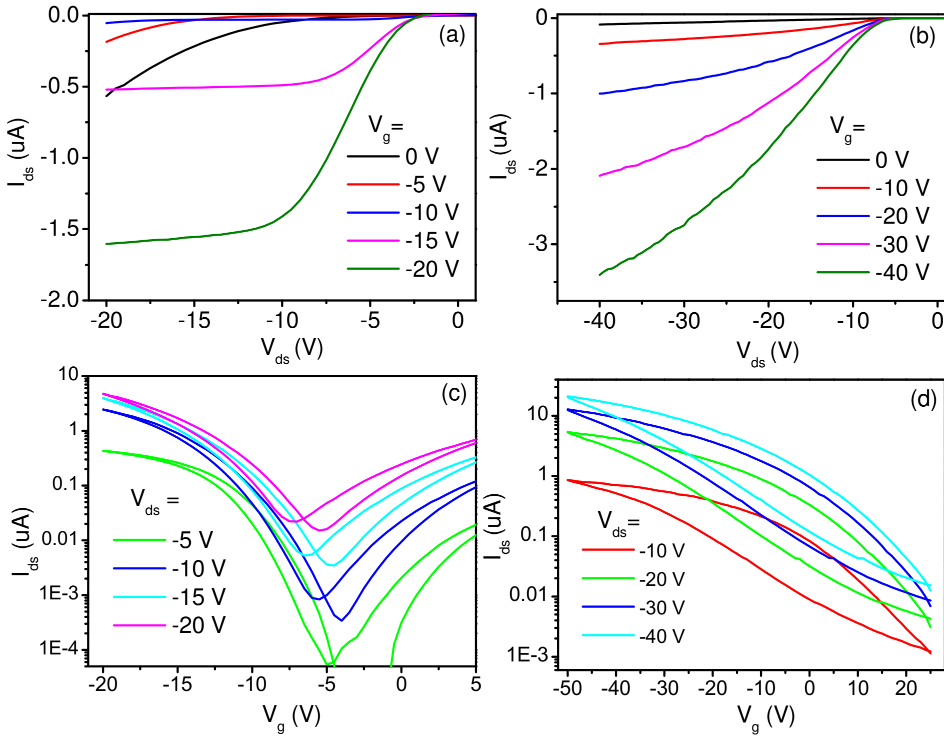

Figure 6.4 Output and transfer curves of the device with 20 μm channel length before (a), (c), respectively, and after annealing in air (b) (d), respectively.

The effect of annealing in air on the electrical performance of SWNT devices was also investigated. Fresh devices without exposure to air were annealed in air at 400 ℃ for 2 h. These are the conditions which have been used by other authors for the removal of the polymer residue. [23] The electrical characteristics of the transistor (20 μm channel length) before and after annealing are shown in Figure 6.4. All ambipolar transistors converted into p-type only devices after the treatment and no mobility improvements were observed. Transfer characteristics of the devices after annealing in air (Figure 6.4(d)) show a hysteresis in current as high as 190 nA (gate bias: -10V), which is much larger than that of the fresh devices ~ 44 nA. This can be due to the destructive effects on the self-assembled molecules with high temperature treatment. Also the influence of residual impurity (e. g. polymer chains carbonization) should not be neglected. The sweeps in all the devices show the hysteresis is advancing in nature instead of retarding. This is the typical sign of the appearance of charge carrier traps in the dielectric layer which is commonly

observed in SWNT transistors. [34] This is a further prove of the necessities of surface modification and water-free sample preparation to obtain ambipolar characteristics in SWNT based transistors.

As we discussed above, a Schottky barrier is present at the SWNT/electrode contact due to the mismatch between the work function of the metal and the conduction (or valence) band of the semiconducting nanotubes. The output characteristics of SWNT transistors (Figure 6.4(a) and 6.4(b)) show nonlinear increase of drain current at low drain voltage, which is a typical feature of injection problems. Another observation is that the conductance of the device after annealing increased compare to that of the freshly made one, but the saturation regime in the output curves (Figure 6.4 (b)) became less pronounced than in the pristine devices (Figure 6.4 (a)). We conjecture that such variation is due to a varied weight of contribution of the Schottky barrier present at the contact (electrode/tube) and of the channel resistance (tube/tube contact). In the case of fresh devices, the percolation of carriers between tubes is the major factor determining carrier transport in SWNT transistors and can be modulated by the gate bias. Annealing treatment indeed reduced barrier between tubes with the removal of the polymer increasing the drain current. However, in this case the contact problem between electrodes and SWNTs plays a more important role. A less pronounced saturation regime in the output characteristics of FETs is then expected as we observed experimentally.

Figure 6.5 Representative SEM image of the device channel region.

Figure 6.5 shows the scanning electron microscopy (SEM) image of the channel. The coverage of the SWNTs is in the range of 0.5-1%, indicating a much higher effective mobility (μ_{eff}) compared to the device mobility reported above. μ_{eff} can be extracted by taking into account of the coverage of SWNTs in the channel region

and the effective gate capacitance (C_{eff}) that differs from the sheet capacitance of the dielectric layer. [35] We estimated the effective channel width to be around 1% of the channel width based on the coverage of SWNTs. By taking into account the realistic electrostatic coupling between nanotubes and the gate electrode, we recalculated using the following equation: [10]

$$C_{eff} = \{C_Q^{-1} + \frac{1}{2\pi\varepsilon_0\varepsilon_{ox}}\ln[\frac{\Lambda_0}{R}\frac{\sinh(2\pi t_{ox}/\Lambda_0)}{\pi}]\}^{-1}\Lambda_0^{-1}$$

Where Λ_0^{-1} stands for the density of SWNTs (3-4 tubes/μm), C_Q is the quantum capacitance of nanotube, ε_{ox} is the dielectric constant of SiO_2, τ_{ox} is the oxide thickness (230 nm) and R is the diameter of the nanotube (in average 0.9 nm). The effective capacitance was calculated to be 2.1 nF/cm^2. We could therefore extract the effective mobility (μ_{eff}) around 6 cm^2/V s, almost three orders of magnitude higher than the device mobility shown above.

6.3 Conclusions

Ambipolar operation has been observed in solution processed SWNT transistors. Device mobility in the range 10^{-3}-10^{-2} cm^2/V s in both p and n channels with elevated on/off ratio was obtained and demonstrate the high purity of the semiconducting SWNT sample used. Effects of the ambient exposure on the electrical characteristics of SWNT FETs were studied. Hole mobility increased with exposure to air and the threshold voltage of the p-channel showed a positive shifts. On the contrary, the n-channel characteristics degraded with air exposure and completely disappear after 24 h. The effect of annealing in air is to convert ambipolar FETs into p type only devices with a larger gate hysteresis. This work points out the origin of the variation of electrical behavior of solution-processed SWNT transistors and further shows the importance of air/water free environments for device preparation.

6.4 Experimental details

Sample preparation

Poly(9,9-di-n-octylfluorenyl-2,7-diyl) (PFO) (MW 58,200 by GPC) was purchased from Sigma-Aldrich (The Netherlands) and CoMoCAT SWNTs were obtained from Southwest Nanotech. The materials were used as received.

The dispersion preparation consisted of a strong sonication and the ultracentrifugation. Dry nanotubes were added to 10 mL of polymer solution in a

weight ratio of 1 mg SWNT to 3 mg polymer, the mixture was sonicated for 4 h in a tabletop ultrasonic bath (VWR, The Netherlands).
After sonication, the crude dispersion was ultracentrifuged at 45k rpm for 1 h (Rotor: MLS-50, 217 000 g). The supernatant (50%) was collected and transferred into new centrifuge tube for the second process in order to enrich SWNTs and to remove excess polymer. The solution was ultracentrifuged at 50k rpm (268 000 g) for 5 h. Over 90% of the dispersed SWNTs precipitated to the bottom of the centrifuge tube, accumulating into a little but visible black 'mat'. The 'mat' was carefully collected and washed with toluene and further subjected to short sonication in toluene, yielding semiconductor-enriched SWNT dispersion.

Optical Characterization
Absorption spectra were recorded with a Perkin-Elmer UV/Vis/NIR spectrophotometer (Lambda 900). For the PL measurements, the SWNT dispersion was excited at 760 nm by a 150 fs pulsed Kerr mode locked Ti-sapphire laser and measured with an InGaAs detectors. The spectra were calibrated for the instrumental response.

Device fabrication
SWNT FETs were fabricated by drop-casting the SWNT solution on bottom-gate/bottom-contact substrates. A heavily doped Si substrate served as the gate electrode with thermally grown SiO_2 used as the dielectric layer (230 nm thickness). The source and drain electrodes consisted of 10 nm of Ti and 30 nm Au. All the substrates were first cleaned in an ultrasonic bath using acetone and isopropanol for 10 min each, and then rinsed with deionized water. Next, the substrates were cleaned with a UV–ozone treatment to remove organic contaminants from the surface. Prior to coating with the SWNT dispersion, the substrate-surface was modified with 3-aminopropyltriethoxysilane (APTES: Sigma-Adrich) in order to increase the adhesion of SWNTs. [36] After the deposition of SWNTs, the substrates were annealed in a vacuum oven at 150 ℃ for 2 h. The device channel was imaged by mean of a scanning electron microscopy (JEOL) at accelerating voltage of 10 kV.

I-V characterization
SWNT FETs were measured either in vacuum or in air ambience (room temperature and humidity 70%) using a Keitley 4200-SCS semiconductor parameter analyzer. The device mobility was calculated from the drain-source current (I_D) versus the gate voltage (V_G) using the formula:

$$\mu = \frac{2L}{WC_i}\left(\frac{\partial\sqrt{I_D}}{\partial V_G}\right)$$

Where L and W are the channel length and width defined by the pattern of the electrodes, C_i is the capacitance per unit surface defined by the thickness of the SiO_2.

References

[1] M. Engel, J. P. Small, M. Steiner, M. Freitag, A. A. Green, M. C. Hersam, Ph. Avouris, *ACS Nano* **2008**, *2*, 2445-2452.
[2] X. Duan, C. Niu, V. Sahi, J Chen, J. W. Parce, S. Empedocles, J. L. Goldman, *Nature* **2003**, *425*, 274-278.
[3] P. L. McEuen, M. S. Fuhrer, H. Park, *IEEE Transactions on Nanotechnology* **2002**, *1*, 78-85.
[4] Ph. Avouris, J. Appenzeller, R. Martel, S. J. Wind, *Proc. IEEE* **2003**, *91*, 1772.
[5] R. Martel, T. Schmidt, H. R. Shea, T. Hertel, Ph. Avouris, *Appl. Phys. Lett.* **1998**, *73*, 2447-2449.
[6] Ph. Avouris, Z. Chen, V. Perebeinos, *Nat. Nanotechnol.* **2007**, *2*, 605-615.
[7] W. J. Yu, B. R. Kang, I. H. Lee, Y.-S. Min, Y. H. Lee, *Adv. Mater.* **2009**, *21*, 4821-4824.
[8] Z. Y. Zhang, S. Wang, Z. X. Wang, L. Ding, T. Pei, Z. D. Hu, X. L. Liang, Q. Chen, Y. Li, L.-M. Peng, *ACS Nano* **2009**, *3*, 3781-3787.
[9] S. Wang, Z. Zhang, L. Ding, X. Liang, J. Shen, H. Xu, Q. Chen, R. Cui, Y. Li, L. -M. Peng, *Adv. Mater.* **2008**, *20*, 3258-3262.
[10] S. J. Kang, C. Kocabas, T. Ozel, M. Shim, N. Pimparkar, M. A. Alam, S. V. Rotkin, J. A. Rogers, *Nat. Nanotechnol.* **2007**, *2*, 230-236.
[11] W. J. Yu, U. J. Kim, B. R. Kang, I. H. Lee, E. -H. Lee, Y. H. Lee, *Nano Lett.* **2009**, *9*, 1401-1405.
[12] S. Fujii, T. Tanaka, Y. Miyata, H. Suga, Y. Naitoh, T. Minari, T. Miyadera, K. Tsukagoshi, H. Kataura, *Appl. Phys. Express* **2009**, *2*, 071601.
[13] T. Tanaka, H. Jin, Y. Miyata, S. Fujii, H. Suga, Y, Naitoh, T. Minari, T. Miyadera, K. Tsukagoshi, H. Kataura, *Nano Lett.* **2009**, *9*, 1497-1500.
[14] H. Wang, J. Luo, A. Robertson, Y. Ito, W. Yan, V. Lang, M. Zaka, F. Schffel, M. H. Rmmeli, G. A. D. Briggs, J. H. Warner, *ACS Nano* **2010**, *4*, 6659-6664.
[15] C. W. Lee, X. Han, F. Chen, J. Wei, Y. Chen, M. B. Chan-Park, L.-J. Li, *Adv. Mater.* **2010**, *22*, 1278-1282.
[16] S. Heinze, J. Tersoff, R. Martel, V. Derycke, J. Appenzeller, Ph. Avouris, *Phys. Rev. Lett.* **2002**, *89*, 106801.
[17] C. M. Aguirre, P. L. Levesque, M. Paillet, F. Lapointe, B. C. St-Antoine, P. Desjardins, R. Martel, *Adv. Mater.* **2009**, *21*, 3087-3091.
[18] J. -Y. Hwang, A. Nish, J. Doig, S. Douven, C. -W. Chen, L .-C. Chen, R. J. Nicholas, *J. Am. Chem. Soc.* **2008**, *130*, 3543-3553.
[19] J. Gao, M. A. Loi, E. J. F. de Carvalho, M. C. dos Santos, *ACS Nano* **2011**, *5*, 3993-3999.
[20] J. Gao, M. Kwak, J. Wildeman, A. Herrmann, M. A. Loi, *Carbon* **2011**, *49*, 333-338.
[21] J. Gao, M. A. Loi, *Eur. Phys. J. B* **2010**, *75*, 121-126.

[22] N. Sturzl, F. Hennrich, S. Lebedkin, M. M. Kappes, *J. Phys. Chem. C* **2009**, *113*, 14628-14632.
[23] N. Izard, S. Kazaoui, K. Hata, T. Okazaki, T. Saito, S. Iijima, N. Minami, *Appl. Phys. Lett.* **2008**, *92*, 243112.
[24] A. Vijayaraghavan, F. Hennrich, N. Stürzl, M. Engel, M. Ganzhorn, M. Oron-Carl, C. W. Marquardt, S. Dehm, S. Lebdkin, M. M. Kappes, R. Krupke, *ACS Nano* **2010**, *4*, 2748-2754.
[25] W. Z. Wang, W. F. Li, X. Y. Pan, C. M. Li, L. -J. Li, Y. G. Mu, J. A Rogers, M. B. Chan-Park, *Adv. Funct. Mater.* **2011**, *21*, 1643–1651.
[26] D. J. Bindl, M. -Y.Wu, F. C. Prehn, M. S. Arnold, *Nano Lett.* **2011**, *11*, 455-460.
[27] E. S. Snow, P. M. Campbell, M. G. Ancona, J. P. Novak, *Appl. Phys. Lett.* **2005**, *86*, 033105.
[28] C. Wang, J. Zhang, K. Ryu, A. Badmaev, L. G. De Arco, C. Zhou, *Nano Lett.* **2009**, *9*, 4285-4291.
[29] C. Lee, C. H. Weng, L. Wei, Y. Chen, M. B. Chan-Park, C. -H. Tsai, K. -C. Leou, P. Poa, J. Wang,L. -J. Li, *J. Phys. Chem. C* **2008**, *112*, 12089-12091.
[30] M. Radosavljević, M. Freitag, K. V. Thadani, A. T. Johnson, *Nano Lett.* **2002**, *2*, 761-764.
[31] A. Javey, M. Shim, H. Dai, *Appl. Phys. Lett.* **2002**, *80*, 1064-1066.
[32] D. Kang, N. Park, J. Hyun, E. Bae, J. Ko, J. Kim, W. Park, *Appl. Phys. Lett.* **2005**, *86*, 093105.
[33] V. Derycke, R. Martel, J. Appenzeller, Ph. Avouris, *Appl. Phys. Lett.* **2002**, *80*, 2773-2775.
[34] W. Kim, A. Javey, O. Vermesh, Q. Wang, Y. Li, H. Dai, *Nano Lett.* **2003**, *3*, 193-198.
[35] Q. Cao, M. Xia, C. Kocabas, M. Shim, J. A. Rogers, S. V. Rotkinb, *Appl. Phys. Lett.* **2007**, *90*, 023516.
[36] M. LeMieux, M. Roberts, S. Barmann, Y. W. Jin, J. M. Kim, Z. Bao, *Science* **2008**, *321*, 101-103.